Impact of Coral Reef Mining Pits on Nearshore Hydrodynamics and Wave Runup During Extreme Wave Events

Klaver, S.; Nederhoff, C. M.; Giardino, A.; Tissier, M. F.S.; van Dongeren, A. R.; van der Spek, A. J.F.

DOI
10.1029/2018JC014165

Publication date
2019

Document Version
Final published version

Published in
Journal of Geophysical Research: Oceans

JGR Oceans

RESEARCH ARTICLE
10.1029/2018JC014165

Impact of Coral Reef Mining Pits on Nearshore Hydrodynamics and Wave Runup During Extreme Wave Events

S. Klaver[1,2,3,4], C. M. Nederhoff[1], A. Giardino[1], M. F. S. Tissier[2], A. R. van Dongeren[1,5], and A. J. F. van der Spek[1,2]

[1]Unit of Marine and Coastal Systems, Deltares, Delft, Netherlands, [2]Department of Hydraulic Engineering, Faculty of Civil Engineering and Geosciences, Delft University of Technology, Delft, Netherlands, [3]Department of Civil and Environmental Engineering, Faculty of Engineering, National University of Singapore, Singapore, [4]Royal HaskoningDHV, Maritime & Aviation, Rotterdam, Netherlands, [5]IHE Delft Institute for Water Education, Delft, Netherlands

Key Points:
- Coral Reef mining pits cause a variation in the nearshore hydrodynamics and wave runup during extreme events
- Pits generally cause a decrease in nearshore wave height and extreme runup mainly due to lower infragravity wave energy
- Pits with a relatively narrow cross-shore width or with a location further from shore are least likely to cause an increase in runup

Supporting Information:
- Supporting Information S1

Correspondence to:
S. Klaver,
klaver.sebas@gmail.com

Citation:
Klaver, S., Nederhoff, C. M., Giardino, A., Tissier, M. F. S., van Dongeren, A. R., & van der Spek, A. J. F. (2019). Impact of coral reef mining pits on nearshore hydrodynamics and wave runup during extreme wave events. *Journal of Geophysical Research: Oceans*, *124*. https://doi.org/10.1029/2018JC014165

Received 11 MAY 2018
Accepted 7 APR 2019
Accepted article online 10 APR 2019

Abstract Small island developing states are among the most vulnerable areas to the impact of natural hazards and climate change. Flooding due to storm surges and extreme waves, coastal erosion, and salinization of freshwater lenses are already a serious threat and could lead to irreversible consequences in the coming decades. Reef flat mining is one of the most common practices to source the required material for the implementation of coastal protection measures, but concerns remain that partial removal of the protective reef could increase wave loading on the islands. However, the available data and knowledge on the effects of these mining pits are currently very limited. This study provides new insights on the effects that pits may have on nearshore hydrodynamics and wave runup. Results are based on a large numerical data set of fringing reefs, derived using the validated XBeach nonhydrostatic+ process-based model. Model results indicate that excavation pits cause a decrease in infragravity wave energy around the fundamental mode of the reef, which is partly caused by reduced wave transmission. Additionally, changes in sea and swell wave energy are attributed to reduced transmission, "a decrease" in wave dissipation, and (triad) wave–wave interaction. Furthermore, in 13% of all modeled cases, an increase in wave runup is observed, mainly due to more sea and swell wave energy reaching the shoreline. This probability is lowest for narrow pits relative to the reef flat width or pits located further from shore.

Plain Language Summary Many small island states are among the most vulnerable areas to the impacts of climate change. Additionally, flooding due to storms, coastal erosion, and loss of freshwater supply already form a serious threat. Mining of dead coral sediments from the reef flat is a common practice to source material for coastal protection works. This could potentially lead to higher waves at the coastline through the partial removal of the reef, which breaks large waves. However, the knowledge on the effects of these mining pits is currently very limited. The present study provides improved explanations on the effects that a pit may have on waves and assesses the resulting risk of flooding it poses on these islands. The results are obtained by simulating a large set of different reefs and wave conditions using a numerical model named XBeach. These show that the effect of a pit can vary significantly, but in general, a pit causes lower waves near the shoreline. At some cases, larger waves at the shoreline were found, thereby increasing the risk of flooding. This risk is the lowest for pits that are located further from the coastline, or those that have narrow width relative to the reef width.

1. Introduction

Small island developing states, and in particular low-lying nations of the Pacific and Indian Oceans, are among the most vulnerable areas to the impact of natural hazards and climate change. The impact of climate change is likely to be increasingly present for small island developing states, as some states face the possibility of losing land area due to its effects, such as coastal erosion and sea level rise (Grady et al., 2013; Storlazzi et al., 2015). Additionally, their small size and remoteness make them increasingly vulnerable to economic and ecological shocks, which is expected to increase with further urbanization and changing climate (Chui & Terry, 2013; Webb & Kench, 2010). Therefore, there is a need for adapting climate change interventions, such as coastal protection, to local capacity and access to resources (Donner & Webber, 2014; Mimura, 1999; Pelling & Uitto, 2001).

A common practice in many coral reef islands as for example in the Marshall Islands, located in the West Central Pacific Ocean, is the use of excavated lithified coral sand and fragments from the reef flats, for the implementation of coastal protection measures or other infrastructure projects (Ford et al., 2013a; Stoddart & Steers, 1977; Xue, 2001). Isolated islands can have a large dependency on reef mining, as alternatives are not economically feasible (Dulby et al., 1995). This practice has been considered as unsustainable in the past, because of slow regeneration of new coral (Smith & Collen, 2004). Moreover, coastal erosion could increase because pits can function as sediment traps (Ford, 2012; Rosti, 1990), can decrease hydrodynamic roughness (Dulby et al., 1995), and can change coastal circulation (Benedet, 2016), resulting in shoreline changes (Bender & Dean, 2003, 2004; Kelley et al., 2004).

Observations and knowledge on the impact of coral reef mining pits on nearshore waves and hydrodynamics remain very limited. A field experiment conducted at Majuro Atoll, Marshall Islands, pointed out that excavation pits on a fringing reef flat can have significant impact on nearshore wave heights and consequently on wave runup (Ford et al., 2013a). More specifically, Ford et al. (2013a) observed that, at this one reef, the excavation caused a decrease in total nearshore wave energy at the beach-toe. The total wavefield was decomposed into two components, the sea-swell waves (SS; $0.04 < f < 0.4$ Hz) and the infragravity waves (IG; $f < 0.04$ Hz). Infragravity waves are bound long waves generated in the shoaling zone by nonlinear interactions between incident SS wave components (Herbers et al., 1994; Longuet-Higgins & Stewart, 1962), and free long waves generated close to the reef crest via the breakpoint forcing mechanism (Péquignet et al., 2014; Pomeroy, Lowe, et al., 2012; Symonds et al., 1982). The observed decrease in wave energy at the beach due to the presence of the pit was mainly explained by a large decrease in infragravity wave energy. Additionally, it was observed that the pit caused a weaker increase in incident SS wave energy.

A numerical wave modeling study of the same reef showed that pit width and cross-shore location can influence the nearshore wave heights (Yao et al., 2016). Yao et al. (2016) also suggested that the decrease in IG wave energy due to the presence of the pit was likely caused by a modification of the two first two natural frequencies of the reef, which could have resulted from a change of the reef open basin structure (Wilson, 1953). The observed increase in SS wave energy at the shoreline was attributed to a decrease in hydrodynamic roughness by removal of the rough reef surface, as well as an increase in water depth that lead to a decrease of breaking induced dissipation (Yao et al., 2016). Payo and Muñoz-Perez (2013) argued that the observed changes in SS and IG energy could be coupled, as a decrease in wave breaking due to the presence of the excavation causes a lower transfer of wave energy from the SS to the IG wave band. Another possible explanation for the decrease in observed (IG) wave energy, which was not discussed in previous studies, is that waves propagating over a deep trench, that is, an excavation pit, are partially reflected, as was found in for instance laboratory experiments conducted by Lee and Ayer (1981).

However, the findings by Ford et al. (2013a) and Yao et al. (2016) are not applicable in a more generic sense, and are likely to change for different reef morphologies, pit designs, and wave conditions. Additionally, Yao et al. (2016) emphasized that further research is needed to understand the broad implications that mining pits can have on the coastal environment. Currently, no assessments have been made on the potential ranges of impacts that reef mining can have on nearshore hydrodynamics and wave runup, related to different reef morphologies, and in combination with different pit designs and offshore wave conditions. Pearson et al. (2017) and Quataert et al. (2015) have shown that both reef morphology and offshore forcing significantly impact nearshore hydrodynamics and wave runup. It is therefore critical to include the possible variations of these parameters in a comprehensive study in order to make more definitive conclusions on the effects of mining pits.

This study aims to generalize and make a more complete assessment of the possible impacts that reef flat mining pits can have on nearshore hydrodynamics. More specifically, this includes the impact on nearshore wave height and wave runup on the adjacent beach during extreme wave events, such as tropical cyclones and highly energetic swell, which are the major sources of flooding toward small island developing states (Giardino et al., 2018; Storlazzi et al., 2018). In particular, the open source process-based wave-resolving hydrodynamic model XBeach nonhydrostatic+ (XBnh+) was used to simulate nearshore hydrodynamics for a large range of reef geometries with and without the presence of the pit, and for different wave conditions. The resulting data set (n = 29,250 simulations) uncovers the mean and possible

ranges of impacts that pits can have on nearshore hydrodynamics, and provides valuable insights on the mechanisms that cause these changes. Moreover, it identifies for which conditions the presence of a pit could lead to higher risk of hazardous situations (i.e., increased runup) and implies possible strategies for mitigation.

The numerical model, including the most relevant input parameters, is described in section 2. The main results are presented in section 3 and discussed in section 4. Conclusions and recommendations are presented in section 5.

2. Materials and Methods

2.1. Model Description

The open-source numerical model XBeach nonhydrostatic+ (XBnh+) was used in order to simulate the nearshore hydrodynamic processes, including flooding and drying of the beach (Roelvink et al., 2009; Roelvink et al., 2018). The nonhydrostatic mode (XBnh) solves the equations of horizontal momentum and mass conservation which resolve both motions in the SS and IG band. The use of the XBnh model has been validated for gravel beaches as well as reef-type coasts (Lashley et al., 2018; McCall et al., 2014; Pearson et al., 2017; Smit et al., 2014). The XBnh+ version of the model adds a virtual pressure layer in the vertical, which improves the frequency dispersion relation in deep water. Therefore, evanescent modes occur less at locations where there are steep bathymetric gradients, such as fore reef slopes and excavation pit walls. A detailed description of the equations that are used in the XBnh+ model is included in the supporting information (see also De Ridder, 2018).

2.2. reef Schematization

The model was set up based on a one-dimensional schematized cross-shore fringing reef (see Figure 1). This includes, moving from offshore to nearshore, a steep fore reef, a reef flat, an excavation pit located on the reef flat, and a sloping beach. The elevation of the bottom topography is given with respect to the mean sea level. The offshore bottom elevation is kept at a constant level throughout this study ($z_0 = -30$ m; $k_{\text{peak}}h < 1.4$) and extended in offshore direction in order to let the model adjust to the boundary conditions. The beach extends from the toe upward to a fictitious elevation of $z_b = 30$ m for all simulations, similar to Pearson et al. (2017), in order to focus on runup as a proxy for overtopping (Matias et al., 2012). Based on Quataert et al. (2015), a distinction is made between the hydrodynamic roughness of the fore reef ($c_f = 0.4$) and reef flat ($c_f = 0.01$) due to characteristic differences in coral reef structure (live/branching coral at the fore reef and deposited/cemented coral sands and fragments on the reef flat and beach). The depth of the excavation pits was set at $z_b = -5$ m, based on measurements by Ford et al. (2013). In order to minimize numerical oscillations caused by the steep pit walls, the wall slope was chosen as 5:1 (compared to near-vertical in real cases). The model outputs were stored at specified locations at (1) the offshore boundary, (2) the top of the fore reef slope, (3) the reef crest (transition between fore reef and reef flat), the center of (4) the reef flat or (5) the pit in case of an excavated reef, and (6) the beach-toe (transition between reef flat and beach; see numbers in Figure 1). Additionally, a numerical runup gauge (7) was used in the model to record the vertical oscillation of the moving waterline. A minimum grid size of $\Delta x = 0.25$ m was used to give stable results. For bottom elevations lower than $z_b = -7$ m, the grid size gradually increases in size in offshore direction with a factor of 1.15 to a maximum value of $\Delta x = 2$ m.

2.3. Varying Input Parameters

A number of parameters were varied to create a large set of artificial reefs with different geometries (Table 1), following the approach of Pearson et al. (2017), Pomeroy, van Dongeren, et al. (2012), and Quataert et al. (2015). The presented parameters were selected based on a sensitivity analysis that assessed the impact of each parameter on reef hydrodynamics and on the effects of excavation pits (Klaver, 2018), as well as on the results of previous research on fringing reef hydrodynamics and wave runup (Pearson et al., 2017; Quataert et al., 2015). Wave runup and subsequent flooding of reef-lined coasts is influenced most by hydrodynamic forcing, fore reef slope, reef width, reef submergence, and beach slope (Pearson et al., 2017; Quataert et al., 2015; Shimozono et al., 2015). The values for these characteristics are in accordance with sources cited in Kolijn (2014) and Quataert et al. (2015). The input variables that were covaried were reef submergence (h_{reef};range 0.5–2.5 m), fore reef slope ($\alpha_{\text{fore reef}}$; range 0.1–0.5), reef flat width (W_{reef}; range

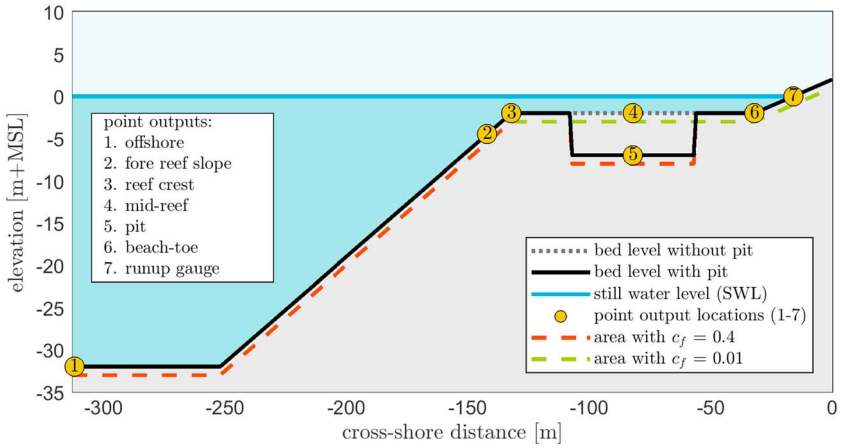

Figure 1. reef schematization and model setup (with and without presence of the pit). The numbers indicate the locations of the output points.

50–450 m), and beach slope (α_{beach}; range 0.05–0.2). Additionally, Google Earth satellite images of different locations in the Marshall Islands were used to measure and obtain a range of values for pit width (W_{pit}; range 6–57% of reef flat width), and cross-shore location of the pit (x_{pit}; range 30–70% of reef flat width, measured from beach-toe; Klaver, 2018).

At the offshore boundary, the model was forced with a JONSWAP spectrum (Hasselmann et al., 1973). Different wave boundary conditions were used and equal to $H_{s,0} = 2.5$, 5.0 m and $T_{p,0} = 16$ s, representative for swell events in the region with a return period equal to 1 and 50 years, respectively, and equal to $H_{s,0} = 7.5$ and $T_{p,0} = 10$ s, representative for a tropical cyclone event with a return period of 50 years (Table 2; Giardino et al., 2018).

By covarying the input parameters, every possible combination of reef geometry and wave conditions was run, amounting to $n = 3 \cdot ((3 \cdot 5 \cdot 5 \cdot 5 \cdot 5 \cdot 5)+(3 \cdot 5 \cdot 5 \cdot 5)) = 29{,}250$ simulations in total. This includes $(3 \cdot 5 \cdot 5 \cdot 5 \cdot 5 \cdot 5) = 9{,}375$ combinations of reef geometries with pit and $(3 \cdot 5 \cdot 5 \cdot 5) = 375$ combinations without. This significantly adds to previous studies by Ford et al. (2013a), whose observations consist of two reef transects, and Yao et al. (2016), who performed a limited amount of numerical simulations (<30) of the same reef.

2.4. Processing of Model Output

Variance density spectra at the output locations were obtained by fast Fourier transform of the surface elevation time series with Hann filter and Welch method. The length of these time series was 6 hr, of which the first hour was discarded to remove spin-up effects from the model results. The spectral resolution that was used was $df = \frac{1}{3{,}600}$ Hz. The number of Welch repetitions was equal to 9. The frequency domain was divided into two: the IG and the SS band, with a split frequency at $f = 0.04$ Hz, based on conventions from previous literature. Significant wave heights were estimated as $H_s = 4 \cdot \sqrt{m_0}$, with m_0, the zeroth-order spectral

Table 1
Reef Geometries Simulated in the Model

Parameter	Symbol	Values						Unit
reef submergence	h_{reef}	0.5	1	1.5	2	2.5		m
Fore reef slope	$\propto_{fore\ reef}$	0.1	0.2	0.3	0.4	0.5		-
reef flat width	W_{reef}	50	150	250	350	450		m
Beach slope	$\propto_{beach}$	0.05	0.125	0.2				-
Pit width	W_{pit}	0	6	19	32	45	57	% W_{reef}
Pit cross-shore location	x_{pit}	30	40	50	60	70		% W_{reef}

Table 2
Wave Input Conditions Simulated in the Model

Extreme Event	$H_{s,0}$ (m)	$T_{p,0}$ (s)
1/1 year swell	2.5	16
1/50 year swell	5.0	16
1/50 year cyclone	7.5	10

moment calculated over a given frequency band. The 2% wave runup $R_{2\%}$ was used as a proxy for overtopping and potential flooding toward the island (Battjes & Schijf, 1972; Holman, 1986; Matias et al., 2012; Wassing, 1957). $R_{2\%}$ is defined as the threshold level above which the highest 2% wave runup levels are found. The same random boundary forcing time series were reused in each simulation, in order to allow for a direct comparison of the different runs.

3. Results and Analysis

3.1. Validation of XBnh+ on Reefs With an Excavation Pit (Field Data)

In order to validate XBnh+ for wave transformation on a fringing reef with excavation pit, model results were compared to observations as described in Ford et al. (2013a) during a field study at Majuro Atoll (the Marshall Islands). This is the only data set currently available describing reef hydrodynamics over an excavation pit. Wave transformation over the reef was assessed at two cross-shore transects, approximately 50 m apart. Transect (t1) includes the presence of a pit, while transect (t2) is characterized by a natural reef with no pit (Figures 2c and 2d). Pressure time series were recorded at four locations on the reef.

Measurements of wave heights and water levels were collected during a 24-hr event on 1 July 2011 at bursts of 30 min (Figures 2a–2d). Offshore water levels varied during the observation period between

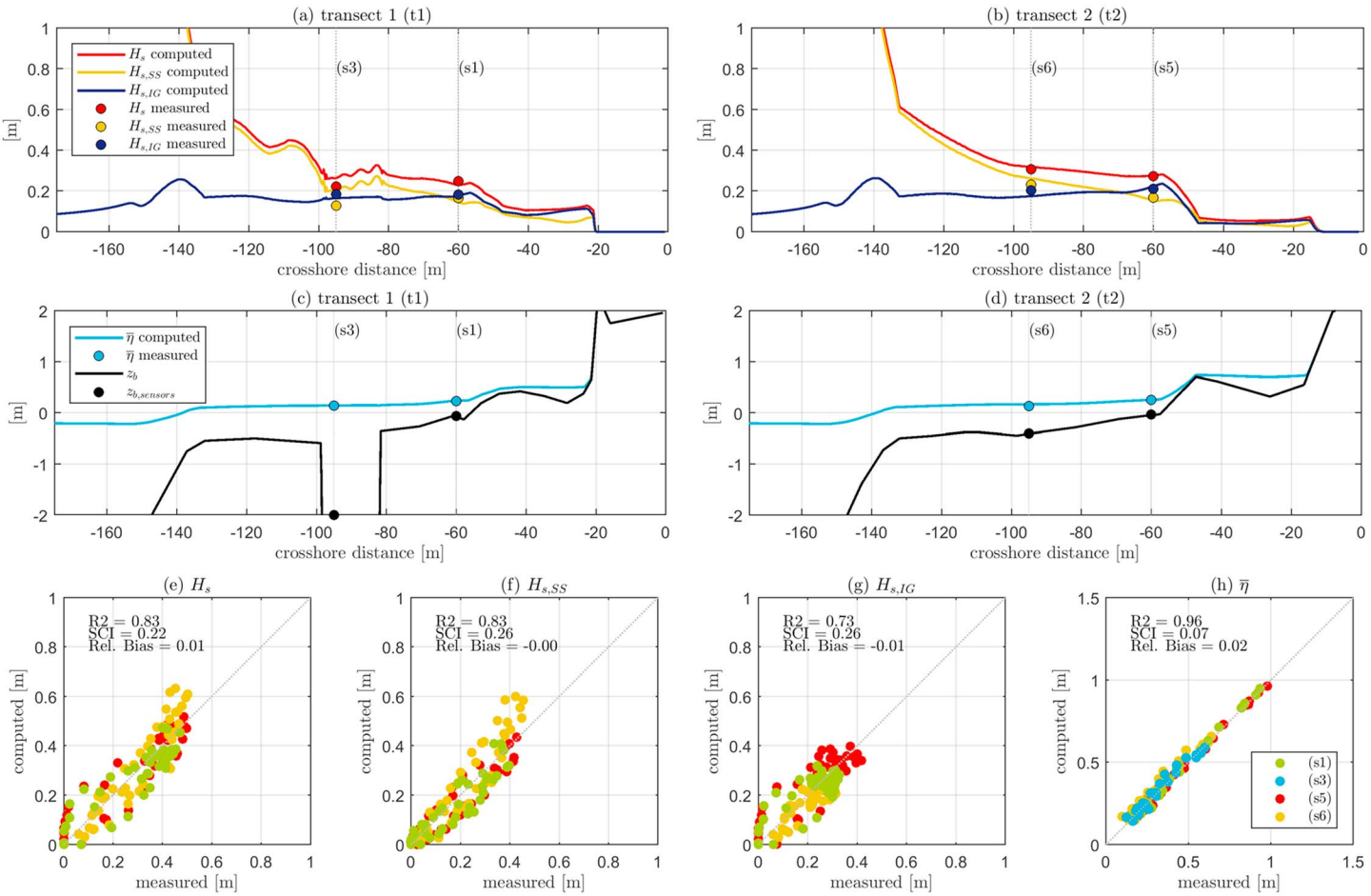

Figure 2. Comparison of modeled and observed wave and water level data across the reef. (a and b) The modeled wave transformation across the reef, respectively, at transects t1 and t2, averaged over the observation period, with measured values indicated by the dots. (c and d) The average water-level transformation across the reef at the same transects. Scatterplots of measured and modeled (e) total wave height, (f) SS wave height, (g) IG wave height, and (h) mean setup at the four sensor locations are shown. Measurements were obtained from Ford et al. (2013a).

−0.8 and + 0.9 m above mean sea level. The event was characterized by shore-normal (southern) swell with an average significant wave height $H_{s,0}$=1.53 m and a mean offshore peak period $T_{p,0}$=10.1 s. Wave conditions were obtained from an offshore wave buoy located 5 km to the east of the measuring site. In absence of more detailed information on the offshore wave spectrum, a JONSWAP spectrum with a peak enhancement factor (γ) of 3.3 was used as input boundary condition. Additionally, bottom friction was chosen to vary spatially, in order to account for the difference in hydrodynamic roughness for the live coral at the reef crest ($c_f = 0.4$, $x < -135$ m; Figures 2c and 2d) and relatively smooth reef flat ($c_f = 0.01$, $x > -135$ m).

The model predictions of wave heights and water levels, averaged over the full duration of the simulation, show a good fit with measurements (Figures 2a–2d). Results show that XBnh+ can predict the wave heights across the reef reasonably well (Figures 2e–2 g). The coefficient of determination (R^2) was estimated equal to 0.73–0.83 at the two transects, the scatter index (Zijlema, 2012) to 0.22–0.26, and the relative bias (Rel.Bias) to ±0.01 for total (Figure 2e), SS (Figure 2f), and IG (Figure 2 g) significant wave heights. Estimates of mean water level were even more accurate with R^2 =0.96, scatter index =0.07, Rel.Bias =0.02 (Figure 2 h). The good fit for the mean water level was however expected, as the (initially unknown) offshore sea level was chosen to maximize the agreement between measured and observed setup on the reef flat. Throughout the duration of the event, average wave-induced setup at sensor 1 (s1) was 0.44 m above mean sea level. A slight overprediction of SS wave height can be observed for the highest waves on the reef flat (corresponding to high water) at sensor 6 (s6; Figure 2f). Wave heights of sensor 3 (s3) have been excluded from the comparison due to errors in the transformation of the recorded pressure signal of this sensor into surface elevation time series. This is possibly caused by inapplicability of linear wave theory at abrupt depth changes (Ford et al., 2013a), which results in an overestimation of significant (SS) wave height at (s3) in XBnh+ (Figure 2b). A possible explanation for the differences between simulated and measured wave heights can be that the boundary conditions used to force the model offshore did not include the effect of locally generated wind waves. Furthermore, because of its location, the buoy is likely to be exposed to waves from different directions compared to the nearshore measuring site. The effect of incoming multidirectional waves is not incorporated in the one-dimensional model. Finally, the bathymetry of the fore reef ($x < -130$ m in Figures 2c and 2d) was inferred by Ford et al. (2013a). Both possible inaccuracies in the bathymetric data and offshore wave conditions are found to have a significant impact on nearshore hydrodynamics (Pearson et al., 2017; Quataert et al., 2015).

Despite of the uncertainties in the measured data set, the XBnh+ model is able to reasonably reproduce the observations by Ford et al. (2013a). When comparing the transect with pit (t1) to the transect with no pit (t2), model results show that shoreward of the pit (Figures 2a and 2b; sensors s1 and s5) there is a decrease in IG wave energy and an increase in SS wave energy. Additionally, there is a slight decrease in mean water level (Figures 2c and 2d).

3.2. Wave Transformation Over a reef Flat With Excavation Pit

The validated model was then used to assess the wave propagation over fringing reefs with pits. In order to explain the impacts that a pit has on nearshore hydrodynamics, results from a first model case are presented in Figure 3. The reef and pit geometry are characterized by $h_{\text{reef}} = 0.5$ m, $W_{\text{reef}} = 150$ m, $\alpha_{\text{fore reef}} = 0.3$, $\alpha_{\text{beach}} = 0.125$, $W_{\text{pit}} = 85.5$ m, and $x_{\text{pit}} = 75$ m. By analyzing incoming and outgoing wave heights at different locations, some relevant nearshore processes can be identified. Incoming and outgoing wave signals were separated using the method described by Guza et al. (1984), which is suitable for shallow water conditions on the reef flat. This method decomposes the time series of the sea surface elevation $\eta(t)$ and the horizontal velocity $u(t)$ into shoreward $PC(t)$ and seaward propagating waves $MC(t)$, by using the following equation:

$$\mathrm{PC}(t) = \left(\eta(t) + \sqrt{\frac{h}{g}}\cdot u(t)\right)\cdot 0.5 \quad \mathrm{MC}(t) = \left(\eta(t) - \sqrt{\frac{h}{g}}\cdot u(t)\right)\cdot 0.5$$

where h is the local average water depth and g is the gravitational acceleration. Incoming wave signals with and without the presence of the pit were identical up to the location of the pit (see Figures 3a, 3c, and 3e, with pit located at $x \approx -360$ m). For the unexcavated case, the incoming SS wave height (Figure 3c) decreases over the entire reef flat. This attenuation of incoming SS waves is the result of wave breaking and, to a

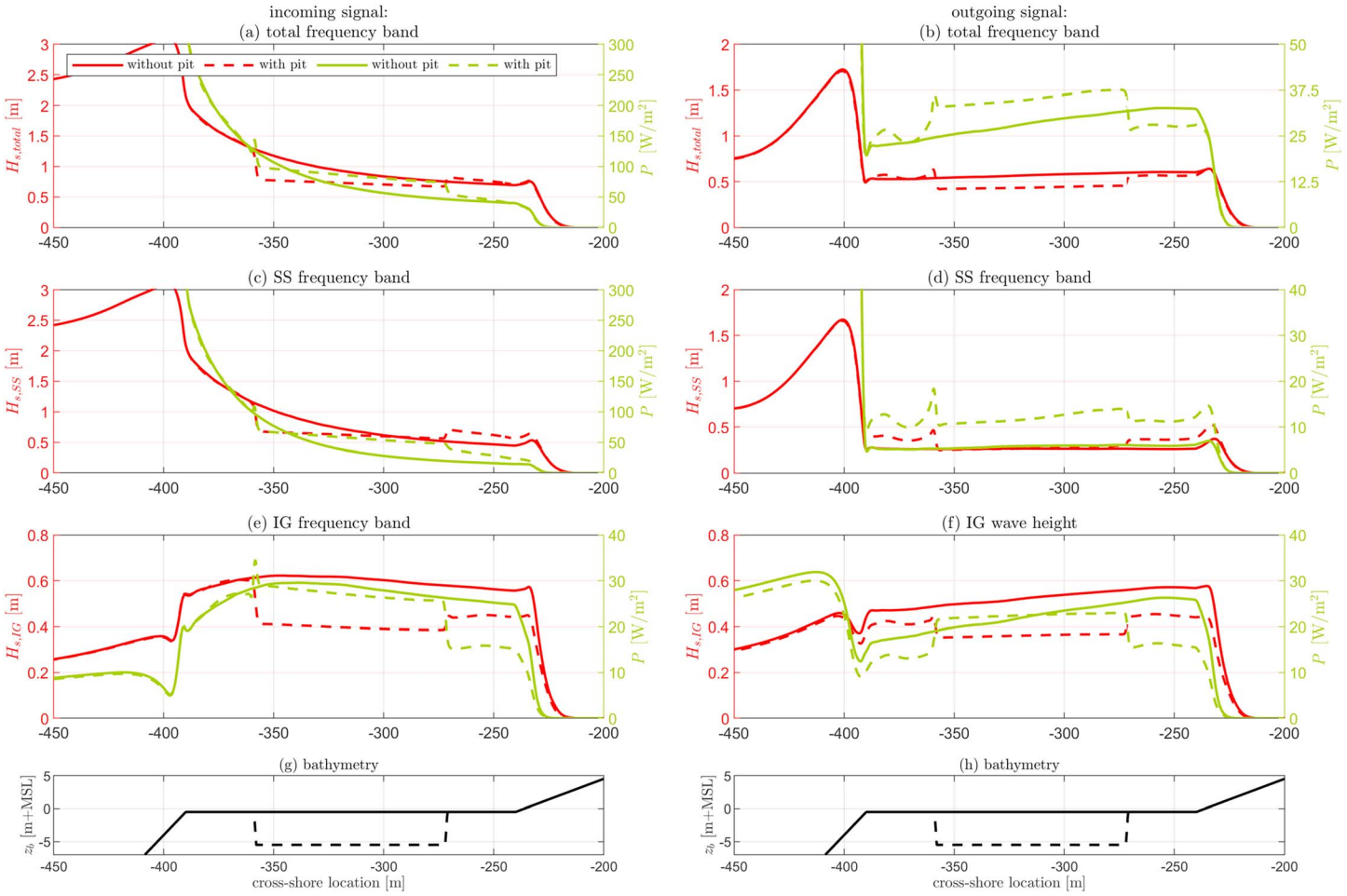

Figure 3. Simulated wave heights (left axis, red) and wave energy fluxes (right axis, green) over a reef with (dashed lines) and without (solid lines) excavation pit, separated into incoming (left subplots) and outgoing (right subplots) signals (Guza et al., 1984). (a and b) The significant wave height and energy fluxes computed over the total frequency domain, (c and d) the SS wave height and energy fluxes, (e and f) the IG wave height and energy fluxes, and (g and h) the bottom topography of both reefs.

lesser extent, bottom friction (Lowe et al., 2005; Monismith et al., 2015; Pearson et al., 2017). The minor role played by bottom friction in the observed dissipation was demonstrated by comparing the model outputs with additional simulations without bottom friction (not shown). The increase in incoming IG wave energy on the outer reef (Figure 3e) suggests that energy transfers from the SS to the IG wave band through triad wave–wave interactions also contribute to the decrease in SS wave energy on the outer reef, which is in agreement with previous studies (Nwogu & Demirbilek, 2010). The process of triad interactions exchanges energy between three interacting wave modes (subharmonics and superharmonics) and occurs in shallow and intermediate water depth (Madsen & Sorensen, 1993). The phase mismatch between the bound and free waves numbers govern the strength of the interactions. This implies that for decreasing water depth, which causes waves to become nondispersive, the process will be enhanced. At the adjacent beach (IG) waves are reflected, which can lead to a standing wave pattern on the reef flat (Cheriton et al., 2016; Gawehn et al., 2016; Pomeroy, van Dongeren, et al., 2012).

For the excavated case, a local decrease in the incoming wave height is observed at the location of the pit ($-360 < x < -275$ m; Figures 3a, 3c, and 3e), which is mainly the result of deshoaling due to locally increased water depth. Partial reflection of the incoming waves in the offshore direction by the pit also contributes to the decrease in incoming wave height over the reef flat, as demonstrated by the sharp decrease in the total incoming energy flux at the edges of the pit (Figure 3a., green dashed line). Despite the partial reflection associated to the pit, the incoming SS wave height reaching the beach is 28% larger for the

excavated case (Figure 3c; $x \approx -240$ m). This is mainly due to the decrease in breaking-induced dissipation over the excavated reef. Analyses of the model outputs have indeed showed that the number of breaking waves, identified as the waves for which the breaking module was activated during the XBeach-NH+ runs, decreased by more than 30% over the pit.

Additionally, there is less nonlinear energy transfer from SS to IG waves due to locally increased water depth, which decreases SS forcing over the pit and limits IG wave growth on the reef flat (Figure 3e). This results in a larger dissipation rate of IG wave energy over the pit (Figure 3e, green lines), and therefore lower IG wave energy at the shoreward pit boundary, compared to a reef without pit. There is a significant decrease in wave energy flux at the shoreward pit wall, where IG waves are partially reflected and decrease 23% in height. This is comparable to an analytical reflection coefficient of $K_r = 0.35$ for IG waves travelling over such a step from deep to shallow water when linear wave theory is assumed (Dean and Dalrymple, 1991). The net effect on the wave height at the beach depends on the relative importance of these processes. For the case considered here, the presence of the pit leads to larger SS waves at the beach-toe (Figure 3c; $x = 240$ m), and lower IG wave height (Figure 3e; $x = 240$ m). The combined effect is a minor increase in incoming total nearshore significant wave height at the beach-toe (Figure 3a; $x \approx -240$ m) in presence of the pit.

The difference between the outgoing and incoming energy fluxes at the reef crest ($x \approx -390$ m) can be used to estimate the energy dissipated over the reef flat. As the total incoming energy flux (Figure 3.2a) is the same at $x \approx -390$ m for the cases with and without pit, the difference in the outgoing energy flux (Figure 3.2b) between the two cases can be attributed to changes in energy dissipation caused by the presence of the pit. The higher outgoing wave height, and thus outgoing energy flux, that is observed for the reef with pit (Figure 3b) confirms that less energy is dissipated in the entire system in the excavated case. More specifically, there is more wave energy present in the SS band and less in the IG band, compared to an unmodified reef (Figures 3d and 3f).

The same reef was used to assess the impact of pit width ($W_{\text{pit}} = 6$ % ,32 % ,57% of W_{reef}) and location ($x_{\text{pit}} = 30$ % ,50 % ,70% of W_{reef}) on the shoreward propagating SS and IG waves. Both pit width (Figure 4) and pit location (Figure 5) have significant impact on shoreward propagating SS (a) and IG (b) waves, and a minor impact on mean water levels (c). In this case, wider pits increase the SS wave height and decrease the IG wave height shoreward of the pit (see Figures 4a and 4b for $x > -270$ m). For wider pits, SS waves dissipate less through depth-induced breaking as they propagate up the fore reef slope and onto the reef flat (Figure 4a). In this process, energy is transferred less to IG wave components (Figure 4b). The combined effects of partial wave transmission (through partial wave reflection) at the shoreward pit wall and decreased wave breaking and wave energy transfer over the pit can result in either an increase (blue line) or a decrease (red line) in SS wave energy. Additionally, there is a decrease in mean water level shoreward of the pit in the order of a few percent. The variations in radiation stresses caused by wave breaking result in wave-induced setup. These variations change due to less wave breaking caused by the presence of a pit, resulting in a lower mean water level compared to an unexcavated reef. This effect is amplified by an increase in width of the pit.

Similarly, a pit located closer to the reef crest increase the SS wave height and decrease the IG wave height shoreward of the pit (see Figures 5a and 5b for $x > -260$ m). These results suggest that the location of the seaward pit edge and the pit width control the relative importance of SS and IG wave heights at the shore. For the more seaward locations of the pit edge, the SS wave breaking stops earlier, conserving more of the SS wave energy which is then higher at the beach (Figure 5a, blue line). Conversely, the IG wave generation also stops earlier, resulting in lower IG waves at the shore (Figure 5b, blue line). However, for pit locations located well away from the reef edge, IG wave heights saturate before the pit edge (Figure 5b, green and red lines) and the more seaward pit locations have little effect on IG wave height at the beach. Both the variation of pit width and pit cross-shore location provide significant insights on the impacts of a pit. However, as suggested by Yao et al. (2016), the effects of pits on nearshore wave hydrodynamics are too case-dependent to formulate any generalized impacts based on the simulation of a single reef.

3.3. Impact on Variance Density Spectra and Wave Heights at the Beach-Toe

In order to assess the general impact that excavation pits can have on nearshore wave height, the outputs at the beach-toe of the full XBnh+ data set ($n = 28{,}125$ runs) are presented and discussed here, by directly

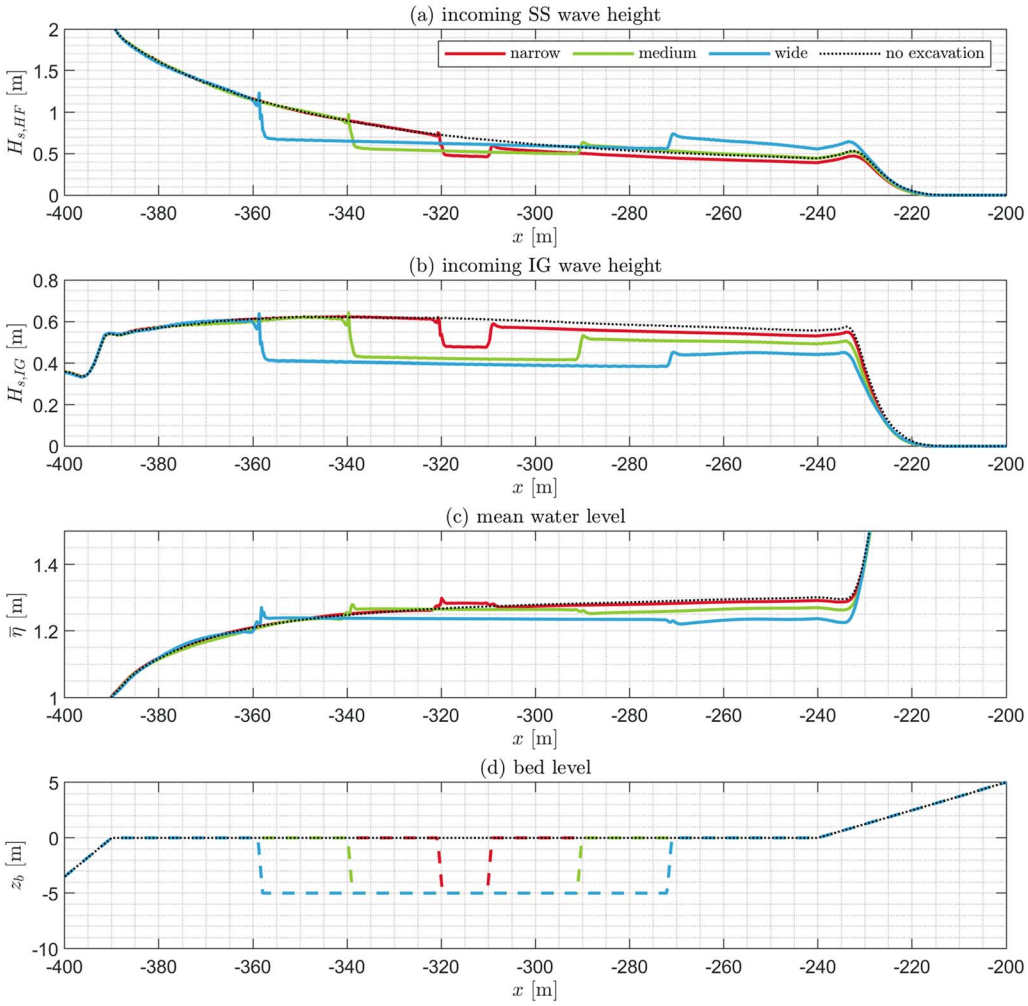

Figure 4. Transformation of shoreward propagating (a) SS and (b) IG waves, (c) mean water levels, and (d) bed levels, for reefs with a narrow (red), medium (green), and wide (blue) pit, compared to a reef without pit (black dotted line).

comparing identical reefs with and without an excavation pit. The variance density spectra of each output location of all the simulations in the data set are determined as discussed in section 2.4. The average of all variance density spectra at each model output location is used to generalize the data set. On average, nearshore wave energy at the beach-toe is dominated by IG frequencies (Figure 6a). Additionally, smaller peaks are located around the offshore peak forcing frequencies ($f \approx 0.06$ Hz,$f \approx 0.1$ Hz). As was observed by Ford et al. (2013a), the effect of an excavation pit changes for different wave frequencies. On average, a reef with pit experiences a large decrease in wave energy in the IG band (see Figure 6b), compared to an identical reef without pit. Moreover, the pit causes an average increase in variance around the offshore peak frequencies, hereafter referred to as the SS peak band ($0.04 < f < 0.125$ Hz). Higher wave frequencies in the SS band ($f > 0.125$ Hz), hereafter referred to as the SS tail, experience a decrease on average. The majority (96%) of the modeled reefs shows a decrease in total wave energy due to the presence of a pit (see Figure 6c). Averaged over all simulations, a pit causes a decrease of 8.5% in total wave height at the beach-toe, a decrease of 2.5% in SS wave height (which consists of an average increase of 1.5% for the SS peak and a decrease of 7.1% for the SS tail), and a decrease of 11.5% in IG wave height. However, a significant spread is observed in the modeling results. When excluding outliers, changes in SS wave height range between −26% and + 20%, changes in IG wave height between −30% and + 8%, and changes in total wave height between −19% and + 3%. Moreover, in nearly all cases (96%) there is a decrease in mean water level shoreward of the excavation (average decrease of 1.5% and

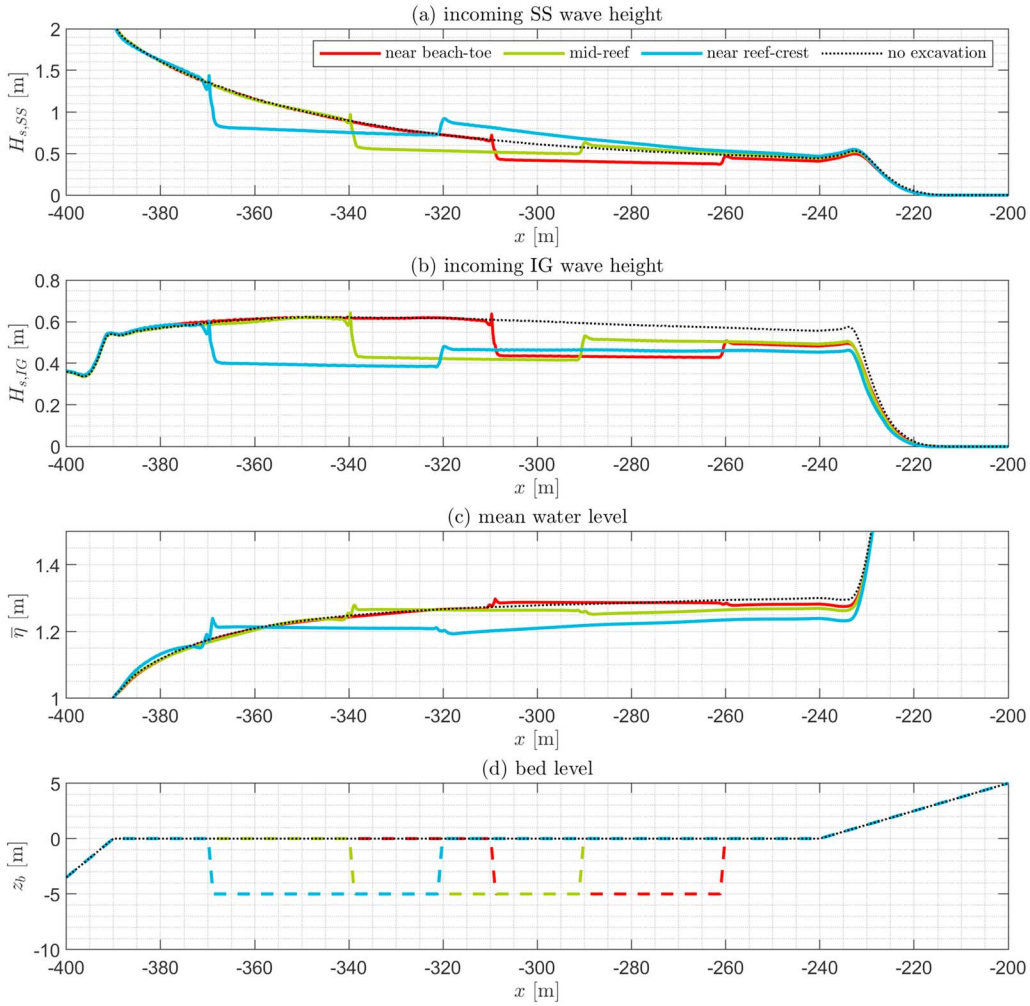

Figure 5. Transformation of shoreward propagating (a) SS and (b) IG waves, (c) mean water levels, and (d) bed levels, for reefs with a pit near the beach-toe (red), midreef (blue), and near the reef crest (blue), compared to a reef without pit (black dotted line).

a range between −5% and + 1%). The impacts of a pit on the SS and IG bands are further elaborated in the two following subsections.

3.4. Impacts of Pits on Wave Runup

In this section the general impacts of excavation pits on wave runup are assessed, as this is a typical indicator of potential wave-induced flooding. The output of the runup gauge in the XBnh+ model was used to compute the $R_{2\%}$ for each simulation. The average effect of an excavation pit is to cause a decrease in runup of approximately 3.6%, with a large spread ranging between −23% and + 13% (Figure 7a). However, there is a distinctive generic effect, as the majority of all modeled reefs experience a decrease in runup due to the presence of a reef flat excavation (~87% of all cases). The results indicate that for an increased severity of wave conditions (i.e., larger and longer waves), the excavation pit has a more substantial impact on decreases in IG wave height. Moreover, the percentage of simulations with an increased runup due to the presence of the pit decreases as well. An explanation for the change in runup due to the presence of the pit can be found by comparing the mean change in variance density of the waterline for reefs that experienced an increase and decrease in runup. The average decrease in runup is caused by less IG wave energy present in the runup signal, which is an important factor that influences wave runup on the beach. Reefs with an increase in runup due to the presence of the pit generally have higher increases in variance around the SS peak in the runup signal, compared to reefs that experience a decrease in runup (see Figure 7b). Moreover,

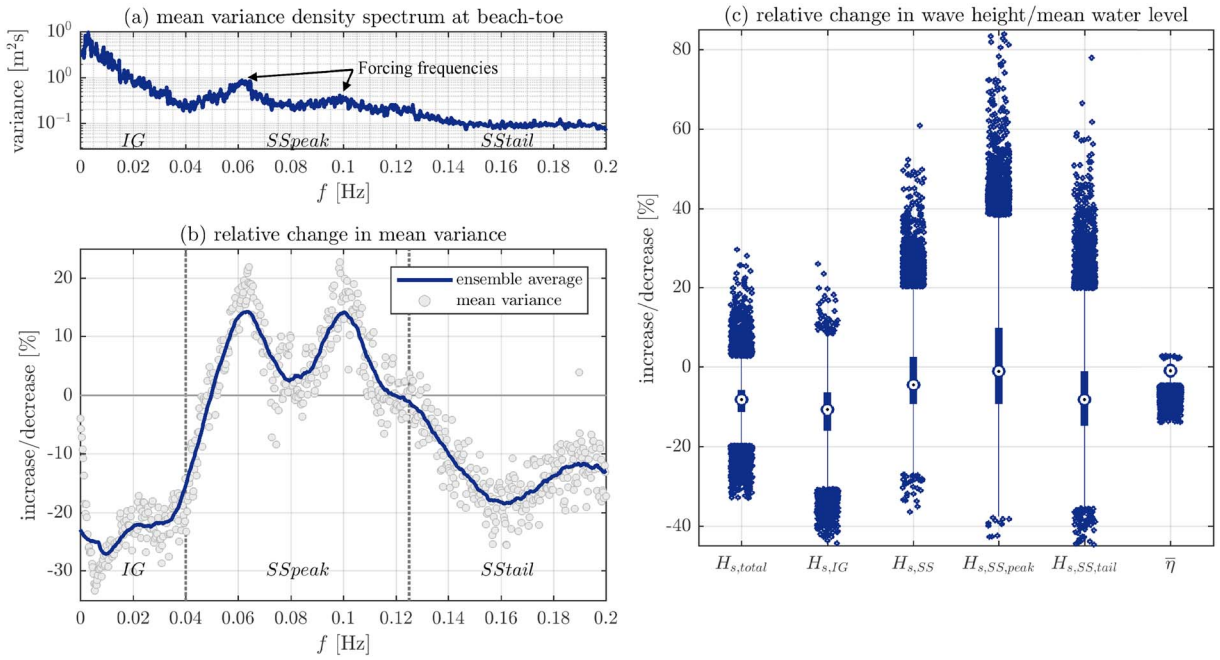

Figure 6. (a) Mean variance density spectrum at beach-toe (averaged over all simulations). (b) Relative change in mean variance at the beach-toe due to the presence of the pit $\left(\sum_{i=1}^{N} S_{pit,i}(f)\right) / \left(\sum_{i=1}^{N} S_{no\ pit,i}(f)\right)$ (grey dots). The purple line shows the ensemble average of the points. The three frequency bands (IG, SS peak, and SS tail) are also indicated. (c) Box plots of the relative change in nearshore significant wave heights and mean water level at the beach-toe due to the presence of a pit, by comparing identical reefs with and without pit. Mean values are represented by the black dots in the white circle. The 25th and 75th percentiles are indicated by the edges of the narrow purple boxes. The purple thin whiskers extend to 1.5 times the interquartile distance, outside of which outliers are shown as purple dots.

there is a lower/larger decrease in IG/SS tail variance, respectively, for reefs with increased runup, compared to reefs with decreased runup. The increased SS peak can be explained by changes in wave dissipation and (triad) wave–wave interaction, which also causes the further decrease in wave energy in the SS tail band. The changes in SS tail energy at the waterline are expected to be of minor influence on the wave runup, compared to changes in wave energy in the IG and SS peak bands.

Regarding the different modeling parameters, the results show that an increase in severity of extreme swell or storms will decrease the probability of an increase in runup ($P(R_{2\ \%,pit} > R_{2\ \%,no\ pit})$; Figure 8a). For an increase in beach steepness (Figure 8b) there will be an increased probability of higher wave runup. An increase in reef submergence (Figure 8c) causes an increase in wave runup to become less probable. For larger reef width, there is a slight increase in probability of an increase in runup (Figure 8d). A steeper fore reef slope results in a lower probability of an increase in runup due to the presence of a pit (Figure 8e). For pit geometry, increasing pit width and cross-shore distance from the reef crest both lead to a larger probability of an increase in runup (Figures 8f and 8g).

4. Discussion

For clarity, discussion points have been grouped under four main topics. In particular, to get a better understanding of the effects that pits may have on: SS wave energy, IG wave energy, wave runup, and other possible coastal management implications.

4.1. Impact on SS Wave Energy

The data set derived from the XBnh+ simulations shows that a large spread in results may be expected in terms of possible impacts of excavation pits on nearshore hydrodynamics and wave heights. However, the mean changes in nearshore wave heights related to the presence of the pit can be related to three main nearshore hydrodynamic processes: wave transmission, wave dissipation (mainly through wave breaking), and (triad) wave–wave interaction.

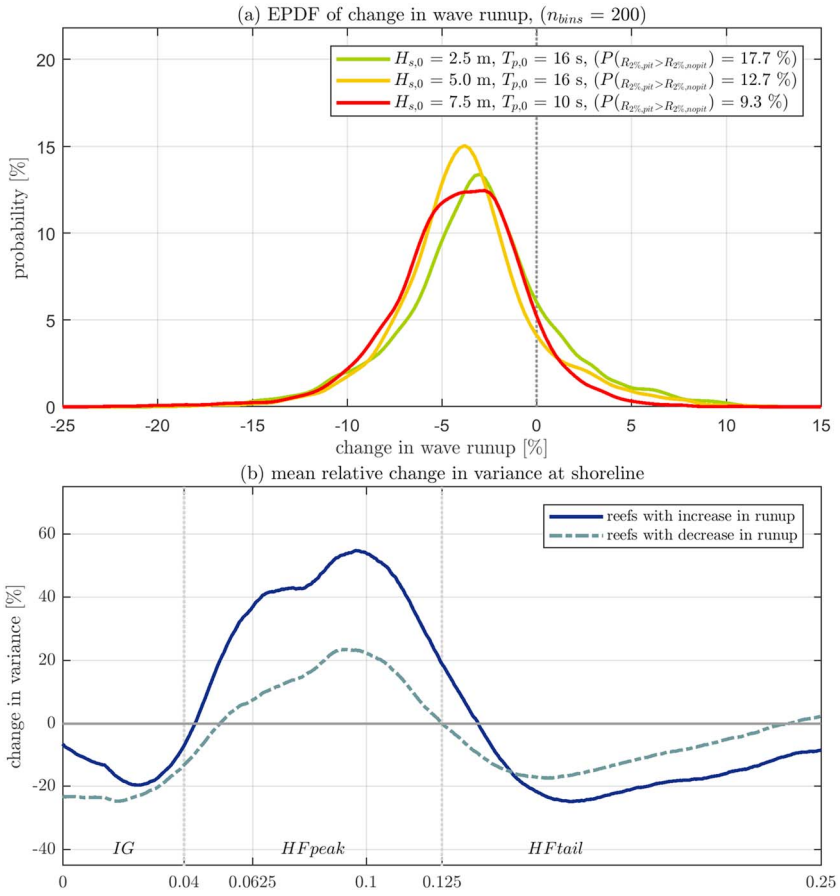

Figure 7. (a) Empirical probability density functions (EPDFs) of the change in $R_{(2\%)}$ due to the presence of the pit, for the three different offshore wave conditions (swell conditions with a return period of 1 year (green) and swell (yellow) and tropical cyclone (red) conditions with a return period of 50 years). (b) Mean relative change in variance at the waterline due to the presence of a pit.

Partial wave transmission over the pit, similar to the findings of Lee and Ayer (1981), causes a decrease in SS wave height at the beach-toe, which is observed in the majority (68%) of all cases. Additionally, variations in the change in SS wave height due to the presence of the pit are the result of decreased wave dissipation and (triad) wave–wave interaction, which both cause an increase in SS peak wave height at the beach-toe. Due to decreased nonlinearity associated with larger water depths (i.e., when a pit is present), both wave breaking and wave–wave interaction decrease (Young & van Vledder, 1993). This decrease in wave dissipation due to the presence of the pit causes an increase in wave energy in the entire SS band. Additionally, due to less energy transfer from the SS peak to SS tail through triad nonlinear wave–wave interactions, there is increased wave energy in the SS peak band and decreased wave energy in the SS tail band. For increasing pit width, relative to the reef flat width, SS wave height also increases compared to narrow pits (Figures 9a and 9b), which generalizes findings from Yao et al. (2016). Wider pits result in larger wave heights in both the SS peak and SS tail bands compared to narrow pits, mainly due to less wave breaking and to a lesser extent due to lower transfer of wave energy from the SS to the IG band. Wave heights in the SS peak band are however more highly affected by changes in pit width than wave heights in the SS tail. This may be related to a combination of changes in wave dissipation and (triad) wave–wave interactions. This is also supported by the change in mean variance at the waterline, where wider pits cause a larger increase/decrease in variance in the SS peak/tail bands, respectively, which implies changes in wave dissipation and (triad) wave–wave interaction (Figure 9c).

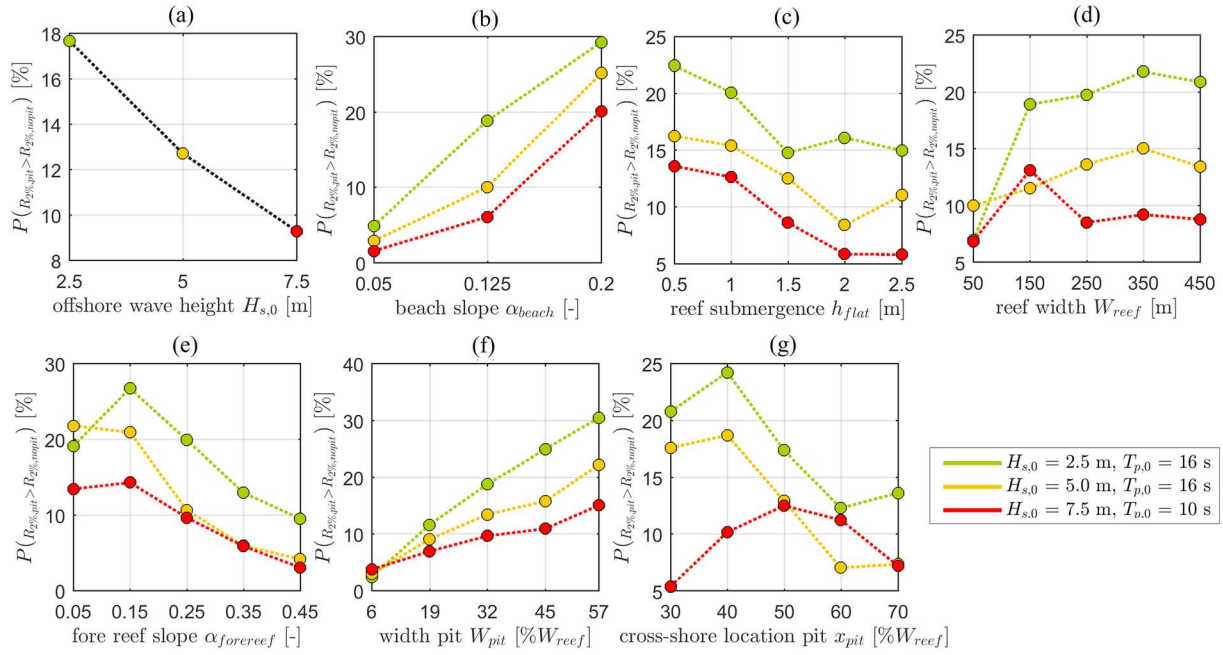

Figure 8. (a–g) Probabilities on an increase in runup as a function of the modeling parameters. Each modeled wave condition is plotted in a different color (swell conditions with a return period of 1 (green) and swell (yellow) and tropical cyclone (red) conditions with a return period of 50 years).

4.2. Impact on IG Wave Energy

Nearly all simulated reefs (98%) showed a decrease in IG wave energy at the beach-toe. Ford et al. (2013) discussed that a possible explanation for the observed decrease in IG wave energy may be a disruption of the quasi-standing wave pattern of IG waves caused by the presence of the pit. Yao et al. (2016) further argued that this decrease may be caused by a modification of the one-quarter and three-quarter wavelength IG standing modes, when considering an ideal open basin. This could suggest that there is an alteration of the natural frequencies of the reef due to the modification of the reef flat. In the modeled data set there is a significant correlation (R^2=0.62; Figure 10c) between the change in IG wave height and the change in wave height around the lowest natural frequency of the reef ($H_{s,f_{n,0}}$). The latter is estimated by integrating the variance density spectrum from $f = 0.9 \cdot f_{n,0}$ to $f = 1.1 * f_{n,0}$, where $f_{n,0} = (1 + 0)/4 \cdot \sqrt{gh}/W_{\text{reef}}$

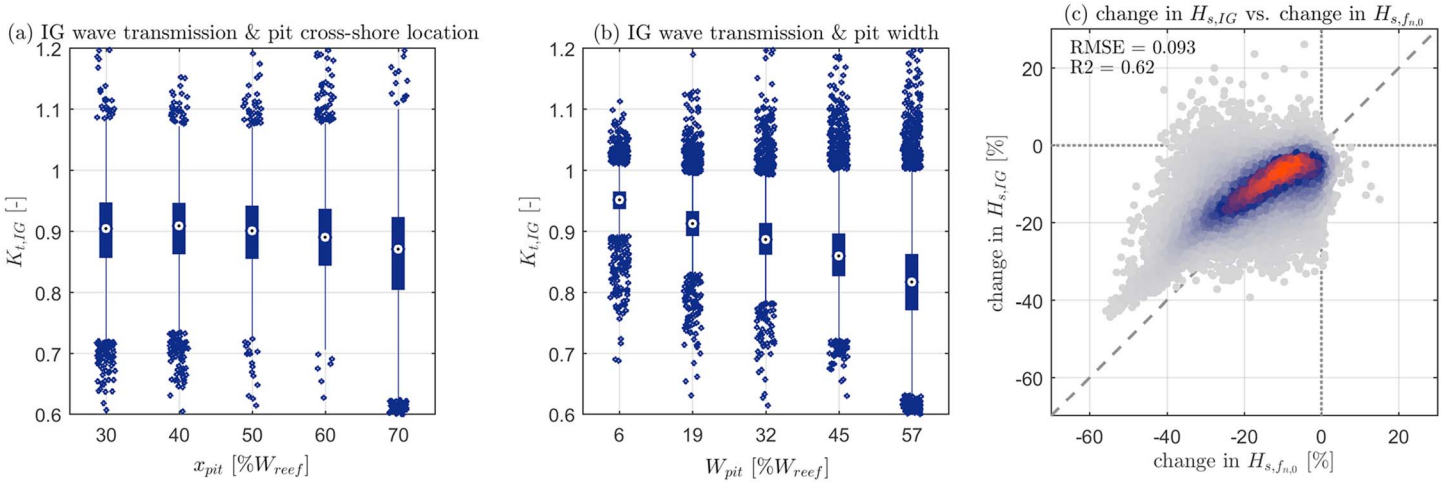

Figure 9. (a and b) Box plots of change (increase/decrease) in (a) SS peak and (b) SS tail wave height at the beach-toe, as a function of pit width relative to reef flat width. (c) Relative change in mean variance at the waterline for two different pit widths, obtained from the runup signal.

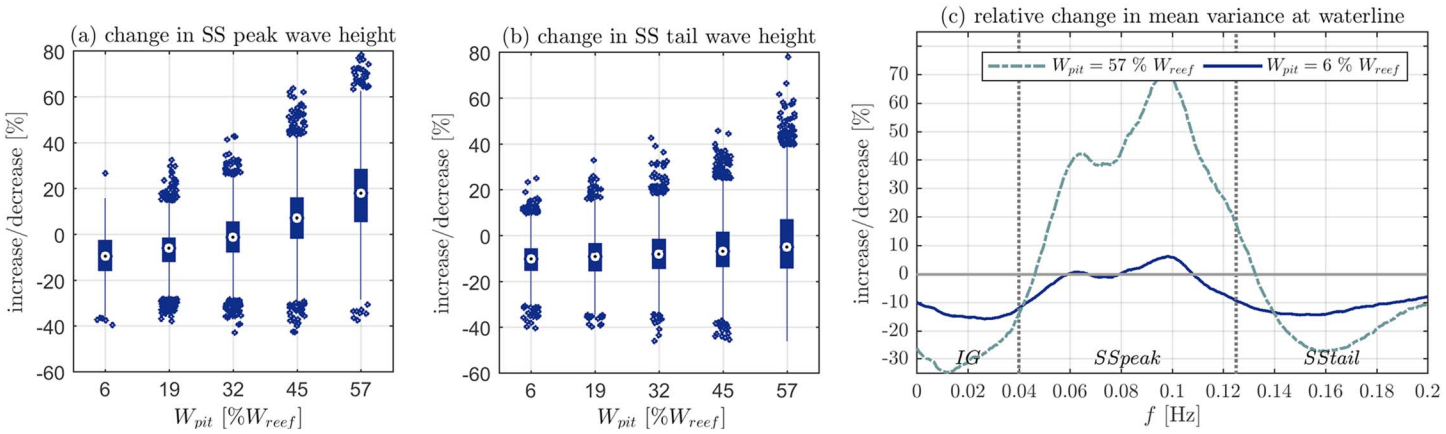

Figure 10. (a and b) Box plots of transmission coefficients of incoming IG wave height, as a function of the cross-shore location and width of the pit. High values of x_{pit} indicate a location relatively closer to the reef crest. (c) Density scatterplot showing the relative change in IG wave height for the case with and without pit, as a function of the relative change in wave height around the lowest natural frequency of the reef ($f_{n,0}$). Density of plotted data increases from grey (outliers) to red (bulk of plotted data).

An alternative explanation may be that waves propagating over a relatively deep trench (i.e., pit) on a horizontal bed (i.e., reef flat) decrease in height due to partial transmission (Lee & Ayer, 1981). The majority (96%) of all simulations shows a transmission coefficient of IG waves, defined as the incoming IG wave height at the leeside of the pit divided by the incoming IG wave height at the same location for an identical reef without pit, lower than 1 (see Figures 10a and 10b). Averaged over the total data set this transmission coefficient is equal to 0.89, slightly larger than values found for small-amplitude regular waves in lab conditions (Lee & Ayer, 1981). Similar to the results of both Kirby and Dalrymple (1983) and Lee and Ayer (1981), the width of the excavation pit has a strong impact on the transmission of IG waves (see Figure 10b).

Also, for larger distance from beach-toe to the center of the pit (x_{pit}, given as percentage of reef flat width), the IG transmission decreases (Figure 10a). This is most likely caused by less IG wave generation through nonlinear energy transfer at the surf zone on the outer reef flat and could explain the lower probability of an increase in runup for these pits (Henderson et al., 2006). A negative correlation between the change in SS wave height and the change in IG wave height over the reef flat ($R = -0.58$) suggests that there is significant wave energy transfer between these two frequency bands. Payo and Muñoz-Perez (2013) argued that the decrease in IG wave energy caused by the presence of the pit could be due to lower energy transfer from the SS band, associated with less wave breaking. This change in energy transfer could also be an explanation for larger decreases in IG wave energy associated with wider pits.

Both the width and cross-shore location of the pit are found to have a significant impact on the IG wave height at the beach-toe, through a combination of partial wave transmission, changes in wave energy transfer, and a disruption of a quasi-standing wave pattern.

4.3. Impact on Wave Runup

Due to IG dominance at the beach-toe, the total wave height decreases for the majority of all modeled reefs (96%). Because of this, the impact of a pit is to decrease the wave runup in most cases (87%). The remainder of the cases (13%) experienced an increase in runup, which was most likely due to higher levels of wave energy in the SS peak band. This increase in SS peak wave energy could be caused by changes in wave dissipation and (triad) wave–wave interaction due to the presence of the pit. The probability of an increase in wave runup due to the presence of a pit is therefore low. However, it is generally increased for pits that are located closer to the beach-toe or that have a large width compared to the reef flat width. As discussed in section 3.2, wider pits have an increased impact on the change in wave dissipation and wave energy transfer mechanisms (Figure 4) that can lead to an increase in runup. Similarly, pits that are located closer to the beach-toe will have a lower impact on the change in wave energy transfer to the IG band (Figure 5), which can cause higher runup. For identical pit width, an increase in reef flat width will decrease the probability of an increase in runup. Additionally, increased reef submergence (e.g., caused by sea level rise) decreases the

probability of an increase in runup, because the impact of a pit on wave propagation over a reef flat with relatively deeper water is significantly smaller. Similarly, for increased wave height, and thus increased severity of wave conditions (e.g., extreme swell and tropical cyclones), the impact of bottom topography on nearshore hydrodynamics monotonically decreases, and will thus result in lower probabilities of increases in runup. Variations in incoming peak wave period do not significantly impact this. Additionally, varying beach slope significantly influences the impact that pits have on wave runup, as the possibility of an increase in runup, caused by increased SS peak wave energy, decreases due to SS wave dissipation on gentle slopes. Steep fore reef slopes also decrease this probability compared to gentle fore reef slopes, because they lead to larger IG dominance on the reef flat, which, combined with the decrease in IG wave energy due to the presence of a pit, are the main cause for a decrease in runup.

4.4. Coastal Management Implications

The anthropogenic pressure and need for aggregate material for coastal protection works and other infrastructure projects in small island states, already very high in the present situation, is likely to increase in the future due to impact of sea level rise and possible socioeconomic developments. As pointed out by Ford et al. (2013a, 2013b), and Payo and Muñoz-Perez (2013), a strategy should be adopted to address this, as reef flat mining is expected to continue due to the high costs associated with importing concrete armor units or stones from other countries. This study has shed light on the possible effects that excavation pits may have on nearshore hydrodynamics. Excavation pits may however lead to additional side effects which have not been considered as part of this research, as, for example, on sediment transport patterns and coastal ecosystems.

Although at most simulated cases pits lead to a decrease in wave runup, which was used in this study as a proxy for island flooding, under specific conditions mining pits may also lead to an increase in wave runup. The study has pointed out which parameters and pit designs could be implemented to reduce the negative impact of these pits on wave runup (e.g., narrower pits, pits further from the shorelines, or pits built where reef submergence is larger). The potential effect of pits on sediment transport pattern is another aspect which must be considered with care, especially at locations that are characterized by a sandy shoreline and/or where alongshore sediment transport of loose material is present. At these locations, mining pits could intercept the transport of sediments, leading to a recession of the adjacent shoreline. Additionally, onshore directed sediment transport may be blocked similarly and cause natural accretion rates of the island to decrease locally (Woodroffe, 2008).

These discussions should encourage policy makers and coastal managers to exert caution when opting for the mining of new pits in proximity of urbanized and environmentally sensitive areas. Alternative (and more sustainable) options should be considered specifically at these islands (e.g., importing materials from other islands, use of material from nonurbanized islands, use of concrete units instead of mined material). Additional caution should be taken in view of the large spreading in results depending on the local island and wave conditions, which make some of these results dependent on specific event or site conditions and therefore not easily translatable to other islands.

5. Conclusions

This study elucidates the impacts that reef flat excavation pits may have on nearshore hydrodynamics and wave runup on shorelines of coral fringing reef islands during extreme wave events. After validation on a limited data set of field observations and a data set of lab observations, the wave-resolving model XBnh+ was used to simulate 28,250 possible scenarios with and without pit on a cross-shore transect of a fringing reef.

Variations in the geomorphology and dimensions and location of the mining pits cause a large spread in the nearshore hydrodynamic response. In general—but not in all cases—reef mining pits cause a decrease in IG wave energy, through a combination of partial wave reflection and a disruption of the quasi-standing wave pattern of IG waves. On average, the SS wave energy also decreases due to the partial reflection of waves. However, an increase in SS peak wave energy and a decrease in SS tail wave energy were observed, caused by less wave dissipation and (triad) wave–wave interaction on the reef flat.

This nearshore response has a significant impact on wave runup on the beach. An increase in runup was observed for 13% of all simulations, which suggests that the potential hazards of reef flat excavating related to coastal flooding could be limited. An increase in runup due to the presence of the pit is caused by larger waves around the offshore peak frequency, compared to reefs that experienced a decrease in runup. Reefs characterized by a large submergence, relatively steep fore reef slope, gentle beach slope, or a large width, have lower chances of an increase in wave runup. Similarly, narrow pits and pits located closer to the reef crest are least likely to cause an increase in runup, and could be considered as options to reduce the impact on wave runup.

Finally, one of the major limitations to this study is the lack of comprehensive and reliable measured data in case of fringing reefs with mining pits. As the need of aggregates on atoll islands is increasing due to socio-economic changes and sea level rise, and mining is becoming a common practice to address these issues, it is highly recommended that a comprehensive monitoring campaign will be carried out to further validate and extend the findings of this research.

Acknowledgments
This work was funded by Deltares through the Deltares Strategic Research Programs "Understanding System Dynamics: From River Basin to Coastal Zone" and "Hydro- and Morphodynamics During Extreme Events." We would like to thank Murray Ford (University of Auckland), Janet Becker (Scripps Institution of Oceanography), and Mark Merrifield (Scripps Institution of Oceanography) for sharing the measured field data. Thanks also to Stefan Aarninkhof (Delft University of Technology) for his guidance throughout the larger part of the project, and Matthijs Gawehn (Deltares, Delft University of Technology) for his suggestions and involvement, as well as Stuart Pearson (Deltares, Delft University of Technology) for sharing his experience with the setting up, and analyzing of large quantities of model simulations. An extract from the data sets presented herein are available as a NetCDF (*.nc) file from the following location: http://opendap.deltares.nl/thredds/fileServer/opendap/deltares/publications/Klaver_2018/XB_dataset_extract.nc. The complete data sets can be obtained by sending a written request to the corresponding author.

References

Battjes, J. A., & Schijf, J. B. (1972). *Wave Runup and Overtopping*. The Hague. Rijkswaterstaat, DWW, https://doi.org/uuid:3f10fa6b-5bb8-41e3-a36e-a5e247e26cd1

Bender, C. J., & Dean, R. G. (2003). Wave field modification by bathymetric anomalies and resulting shoreline changes: A review with recent results. *Coastal Engineering*, *49*(1–2), 125–153. https://doi.org/10.1016/S0378-3839(03)00061-9

Bender, C. J., & Dean, R. G. (2004). Potential shoreline changes induced by three-dimensional bathymetric anomalies with gradual transitions in depth. *Coastal Engineering*, *51*, 331–351. https://doi.org/10.1016/j.coastaleng.2004.12.005

Benedet, L. (2016). Processes Controlling Beach Nourishment Performance at Delray Beach, Florida, USA. Delft University of Technology. http://doi.org/10.4233/uuid:aa444a96-7821-4244-ae6e-b2c28c008ef8

Cheriton, O. M., Storlazzi, C. D., & Rosenberger, K. J. (2016). Observations of wave transformation over a fringing coral reef and the importance of low-frequency waves and offshore water levels to runup, overwash, and coastal flooding. *Journal of Geophysical Research: Oceans*, *121*, 3121–3140. https://doi.org/10.1002/2015JC011231

Chui, T. F. M., & Terry, J. P. (2013). Influence of sea-level rise on freshwater lenses of different atoll island sizes and lens resilience to storm-induced salinization. *Journal of Hydrology*, *502*, 18–26. https://doi.org/10.1016/j.jhydrol.2013.08.013

De Ridder, M. P. (2018). Non-hydrostatic wave modelling of coral reefs with the addition of a porous in-canopy model. Delft University of Technology. MSc Thesis. Retrieved from http://resolver.tudelft.nl/uuid:4f738968-be52–4484-af1d-60a0e74fdbab

Dean, R. G., & Dalrymple, R. A. (1991). *Water Wave Mechanics for Engineers and Scientists*. Singapore: World Scientific. https://doi.org/10.1142/1232

Donner, S. D., & Webber, S. (2014). Obstacles to climate change adaptation decisions: A case study of sea-level rise and coastal protection measures in Kiribati. *Sustainability Science*, *9*(3), 331–345. https://doi.org/10.1007/s11625-014-0242-z

Dulby, N. K., Stanwell-smith, D., Darwall, W. R. T., & Horrill, C. J. (1995). Coral Mining at Mafia Island, Tanzania: A Management Dilemma. *Ambio*, *24*(6), 358–365. Retrieved from. http://www.jstor.org/stable/4314367

Ford, M. R. (2012). Shoreline changes on an urban atoll in the central Pacific Ocean: Majuro Atoll, Marshall Islands. *Journal of Coastal Research*, *279*(January 2012), 11–22. https://doi.org/10.2112/JCOASTRES-D-11-00008.1

Ford, M. R., Becker, J. M., & Merrifield, M. A. (2013a). Reef flat wave processes and excavation pits: Observations and implications for Majuro Atoll, Marshall Islands. *Journal of Coastal Research*, *288*(3), 545–554. https://doi.org/10.2112/JCOASTRES-D-12-00097.1

Ford, M. R., Becker, J. M., & Merrifield, M. A. (2013b). Reply to: Payo, A. and Muñoz-Perez, J.J., 2013. Discussion of Ford, M.R.; Becker, J. M., and Merrifield, M.A. 2013. Reef flat wave processes and excavation pits: Observations and implications for Majuro Atoll, Marshall Islands. Journal of Coastal Research. *Journal of Coastal Research*, *290*(3), 1236–1242. https://doi.org/10.2112/JCOASTRES-D-13-00051.1

Gawehn, M., van Dongeren, A. R., van Rooijen, A., Storlazzi, C. D., Cheriton, O. M., & Reniers, A. J. H. M. (2016). Identification and classification of very low frequency waves on a coral reef flat. *Journal of Geophysical Research: Oceans*, *121*, 7560–7574. https://doi.org/10.1002/2016JC011834

Giardino, A., Nederhoff, C. M., & Vousdoukas, M. I. (2018). Coastal hazard risk assessment for small islands: Assessing the impact of climate change and disaster reduction measures on Ebeye (Marshall Islands). *Journal of Regional Environmental Change*, *18*(8), 2237–2248. https://doi.org/10.1007/s10113-018-1353-3

Grady, A. E., Moore, L. J., Storlazzi, C. D., Elias, E., & Reidenbach, M. A. (2013). The influence of sea level rise and changes in fringing reef morphology on gradients in alongshore sediment transport. *Geophysical Research Letters*, *40*, 3096–3101. https://doi.org/10.1002/grl.50577

Guza, R. T., Thornton, E. B., & Holman, R. A. (1984). Swash on steep and shallow beaches. *Coastal Engineering Proceedings*, *1*(19), 708–723. https://doi.org/10.9753/icce.v19.%p

Hasselmann, K., Barnett, T. P., Bouws, E., Carlson, H., Cartwright, D. E., Enke, K., et al. (1973). Measurements of Wind-Wave Growth and Swell Decay during the Joint North Sea Wave Project (JONSWAP). *Ergnzungsheft Zur Deutschen Hydrographischen Zeitschrift Reihe A*, *12*, 95. https://doi.org/citeulike-article-id:2710264

Henderson, S. M., Guza, R. T., Elgar, S., Herbers, T. H. C., & Bowen, A. J. (2006). Nonlinear generation and loss of infragravity wave energy. *Journal of Geophysical Research*, *111*, C12007. https://doi.org/10.1029/2006JC003539

Herbers, T. H. C., Elgar, S., & Guza, R. T. (1994). Infragravity-frequency (0.005–0.05 Hz) motions on the shelf. Part I: Forced waves. *Journal of Physical Oceanography*, *24*(5), 917–927. https://doi.org/10.1175/1520-0485(1994)024<0917:IFHMOT>2.0.CO;2

Holman, R. A. (1986). Extreme value statistics for wave run-up on a natural beach. *Coastal Engineering*, *9*(6), 527–544. https://doi.org/10.1016/0378-3839(86)90002-5

Kelley, S. W., Ramsey, J. S., & Byrnes, M. R. (2004). Evaluating shoreline response to offshore sand mining for beach nourishment. *Journal of Coastal Research*, *20*(1), 89–100. https://doi.org/10.2112/1551-5036(2004)20

Kirby, J. T., & Dalrymple, R. A. (1983). Propagation of obliquely incident water waves over a trench. *Journal of Fluid Mechanics*, *133*(1), 47–63. https://doi.org/10.1017/S0022112083001780

Klaver, S. (2018). Modelling the effects of excavation pits on fringing reefs. Delft University of Technology. MSc Thesis. Retrieved from http://resolver.tudelft.nl/uuid:17620c42-8c1b-491c-b862-f4c1f6c92a48

Kolijn, D. J. (2014). Effectiveness of a multipurpose artificial underwater structure as a coral reef canopy. Delft University of Technology. MSc Thesis. Retrieved from http://resolver.tudelft.nl/uuid:7794dcfc-0971-4646-9ea2-25f8894176c3

Lashley, C. H., Roelvink, J. A., van Dongeren, A. R., Buckley, M. L., & Lowe, R. J. (2018). Nonhydrostatic and surfbeat model predictions of extreme wave run-up in fringing reef environments. *Coastal Engineering*, *137*(October 2017), 11–27. https://doi.org/10.1016/j.coastaleng.2018.03.007

Lee, J.-J., & Ayer, R. M. (1981). Wave propagation over a rectangular trench. *Journal of Fluid Mechanics*, *110*, 335–347. https://doi.org/10.1017/S0022112081000773

Longuet-Higgins, M., & Stewart, R. (1962). Radiation stress and mass transport in gravity waves, with application to 'surf beats'. *Journal of Fluid Mechanics*, *13*(4), 481–504. https://doi.org/10.1017/S0022112062000877

Lowe, R. J., Falter, J. L., Bandet, M. D., Pawlak, G., Atkinson, M. J., Monismith, S. G., & Koseff, J. R. (2005). Spectral wave dissipation over a barrier reef. *Journal of Geophysical Research*, *110*, C04001. https://doi.org/10.1029/2004JC002711

Madsen, P. A., & Sorensen, O. R. (1993). Bound waves and triad interactions in shallow water. *Ocean Engineering*, *20*(4), 359–388. https://doi.org/10.1016/0029-8018(93)90002-Y

Matias, A., Williams, J. J., Masselink, G., & Ferreira, Ó. (2012). Overwash threshold for gravel barriers. *Coastal Engineering*, *63*, 48–61. https://doi.org/10.1016/j.coastaleng.2011.12.006

McCall, R. T., Masselink, G., Poate, T. G., Roelvink, J. A., Almeida, L. P., Davidson, M., & Russell, P. E. (2014). Modelling storm hydrodynamics on gravel beaches with XBeach-G. *Coastal Engineering*, *91*, 231–250. https://doi.org/10.1016/j.coastaleng.2014.06.007

Mimura, N. (1999). Vulnerability of island countries in the South Pacific to sea level rise and climate change. *Climate Research*, *12*, 137–143. Retrieved from http://www.jstor.org/stable/24866008

Monismith, S. G., Rogers, J. S., Koweek, D., & Dunbar, R. B. (2015). Frictional wave dissipation on a remarkably rough reef. *Geophysical Research Letters*, *42*, 4063–4071. https://doi.org/10.1002/2015GL063804

Nwogu, O., & Demirbilek, Z. (2010). Infragravity wave motions and runup over shallow fringing reefs. *Journal of Waterway, Port, Coastal, and Ocean Engineering*, *136*(December), 295–305. https://doi.org/10.1061/(ASCE)WW.1943-5460.0000050

Payo, A., & Muñoz-Perez, J. J. (2013). Discussion of Ford, M.R.; Becker, J.M., and Merrifield, M.A. 2013. Reef flat wave processes and excavation pits: Observations and implications for Majuro Atoll, Marshall Islands. *Journal of Coastal Research,* 29(3), 545–554. *Journal of Coastal Research*, *290*(3), 1236–1242. https://doi.org/10.2112/JCOASTRES-D-13-00051.1

Pearson, S. G., Storlazzi, C. D., van Dongeren, A. R., Tissier, M. F. S., & Reniers, A. J. H. M. (2017). A Bayesian-based system to assess wave-driven flooding hazards on coral reef-lined coasts. *Journal of Geophysical Research: Oceans*, *122*, 10,099–10,117. https://doi.org/10.1002/2017JC013204

Pelling, M., & Uitto, J. I. (2001). Small island developing states: natural disaster vulnerability and global change. *Global Environmental Change Part B: Environmental Hazards*, *3*(2), 49–62. https://doi.org/10.1016/S1464-2867(01)00018-3

Péquignet, A. C. N., Becker, J. M., & Merrifield, M. A. (2014). Energy transfer between wind waves and low-frequency oscillations on a fringing reef, Ipan, Guam. *Journal of Geophysical Research C: Oceans*, *119*, 6709–6724. https://doi.org/10.1002/2014JC010179

Pomeroy, A., Lowe, R., Symonds, G., Van Dongeren, A., & Moore, C. (2012). The dynamics of infragravity wave transformation over a fringing reef. *Journal of Geophysical Research*, *117*, C11022. https://doi.org/10.1029/2012JC008310

Pomeroy, A. W. M., van Dongeren, A. R., Lowe, R. J., Van Thiel de Vries, J. S. M., & Roelvink, J. A. (2012). Low-frequency wave resonance in fringing reef environments. *Coastal Engineering*, *2012*, 1–10. https://doi.org/10.9753/icce.v33.currents.25

Quataert, E., Storlazzi, C. D., Van Rooijen, A., Cheriton, O. M., & Van Dongeren, A. R. (2015). The influence of coral reefs and climate change on wave-driven flooding of tropical coastlines. *Geophysical Research Letters*, *42*, 6407–6415. https://doi.org/10.1002/2015GL064861

Roelvink, J. A., McCall, R. T., Mehvar, S., Nederhoff, C. M., & Dastgheib, A. (2018). Improving predictions of swash dynamics in XBeach: The role of groupiness and incident-band runup. *Coastal Engineering*, *134*(April), 103–123. https://doi.org/10.1016/j.coastaleng.2017.07.004

xRoelvink, J. A., Reniers, A. J. H. M., Van Dongeren, A. R., van Thiel de Vries, J. S. M., McCall, R. T., & Lescinski, J. (2009). Modelling storm impacts on beaches, dunes and barrier islands. *Coastal Engineering*, *56*(11–12), 1133–1152. https://doi.org/10.1016/j.coastaleng.2009.08.006

Rosti, P. (1990). *Circulation and shoreline survey of Majuro atoll, Republic of the Marshall Islands. Coastal Resource Inventory of Majuro Atoll, Republic of the Marshall Islands*. Hawaii: University of Hawaii Sea Grant Extension Service Honolulu.

Shimozono, T., Tajima, Y., Kennedy, A. B., Nobuoka, H., Sasaki, J., & Sato, S. (2015). Combined infragravity wave and sea-swell runup over fringing reefs by super typhoon Haiyan. *Journal of Geophysical Research: Oceans*, *118*, 3114–3127. https://doi.org/10.1002/jgrc.20224

Smit, P. B., Stelling, G. S., Roelvink, J. A., van Thiel de Vries, J. S. M., McCall, R. T., van Dongeren, A. R., (2014). XBeach: Non-hydrostatic model. Retrieved from http://oss.deltares.nl/documents/48999/06b24380-e87f-42ef-8a88-53f02754413e

Smith, R., and Collen, J. (2004). Sand and gravel resources of Majuro Atoll, Marshall Islands. *SOPAC Technical Report 360. South Pacific Applied Geoscience Commission, Suva, Fiji*, 126.

Stoddart, D. R., & Steers, J. A. (1977). The nature and origin of coral reef islands. In O. A. Jones, & R. Endean (Eds.), *Biology and Geology of Coral Reefs, Volume IV: Geology 2* (pp. 60–102). New York: Academic Press, Inc.

Storlazzi, C. D., Elias, E. P. L., & Berkowitz, P. (2015). Many atolls may be uninhabitable within decades due to climate change. *Scientific Reports*, *5*(1), 14546. https://doi.org/10.1038/srep14546

Storlazzi, C. D., Gingerich, S. B., van Dongeren, A. R., Cheriton, O. M., Swarzenski, P. W., Quataert, E., et al. (2018). Most atolls will be uninhabitable by the mid-21st century because of sea-level rise exacerbating wave-driven flooding. *Science Advances*, *4*(4). https://doi.org/10.1126/sciadv.aap9741

Symonds, G., Huntley, D. A., & Bowen, A. J. (1982). Two-dimensional surf beat: Long wave generation by a time-varying breakpoint. *Journal of Geophysical Research*, *87*(C1), 492–498. https://doi.org/10.1029/JC087iC01p00492

Wassing, F. (1957). Model investiguations of wave run-up on dikes carried out in the Netherlands during the past twenty years. *Proceedings of the 6th Coastal Engineering Conference*, *1*(6), 42.

Webb, A. P., & Kench, P. S. (2010). The dynamic response of reef islands to sea-level rise: Evidence from multi-decadal analysis of island change in the central Pacific. *Global and Planetary Change*, *72*(3), 234–246. https://doi.org/10.1016/j.gloplacha.2010.05.003

Wilson, B. W. (1953). The mechanism of Seiches in Table Bay Harbor, Capetown. In *Coastal Engineering*. (pp. 52–78) Chicago, Illinois: Council of Wave Research. https://doi.org/10.9753/icce.v4.4

Woodroffe, C. D. (2008). Reef-island topography and the vulnerability of atolls to sea-level rise. *Global and Planetary Change*, *62*(1–2), 77–96. https://doi.org/10.1016/j.gloplacha.2007.11.001

Xue, C. (2001). Coastal erosion and management of Majuro Atoll, Marshall Islands. *Journal of Coastal Research*, *17*(4), 909–918. Retrieved from http://www.jstor.org/stable/4300250

Yao, Y., Becker, J. M., Ford, M. R., & Merrifield, M. A. (2016). Modeling wave processes over fringing reefs with an excavation pit. *Coastal Engineering*, *109*, 9–19. https://doi.org10.1016/j.coastaleng.2015.11.009

Young, I. R., & van Vledder, G. P. (1993). A review of the central role of nonlinear interactions in wind-wave evolution. *Philosophical Transactions of The Royal Society B Biological Sciences*, (March 1993, *342*(1666), 505–524. https://doi.org/10.1098/rsta.1993.0030

Zijlema, M. (2012). Modelling wave transformation across a fringing reef using SWASH. *Coastal Engineering*, *1*(33), 26–12. https://doi.org/10.9753/icce.v33.currents.26